Chapter 6
Massive Electric Vehicle Charging Involving Renewable Energy

6.1 Introduction

In the world today, fossil fuels are the dominant energy sources for both transportation sector and electricity generation industry. Statistics show that transportation and electricity generation account for over 60% of global primary energy demands [1]. The future solution for the fossil fuels scarcity, as well as the growing environmental problems associated with their wide usage, will most likely involve an extensive use of electric vehicles (EVs) and adopting renewable energy sources for electric energy production [2]. Under such cases, renewable energy supplied EV charging is becoming a popular approach for greener and more efficient energy usage. Since EVs have controllable charging rate, they can be considered as flexible loads in grid system which can benefit the grid system with demand response or load following. Accordingly, charging scheduling of EVs in the presence of renewable energy becomes a practical and important research problem.

A number of technical and regulatory issues, however, have to be resolved before renewable energy supplied EV charging becomes a commonplace. The arrival of EVs and their required energy amount may appear to be random, which increases the demand-side uncertainties. In addition, while renewable energy offers a cheaper and cleaner energy supply, it imposes great challenges to the stability and safety of the charging system because of its high inter-temporal variation and limited predictability. Therefore, the stochastic characteristics of both EVs and renewable energy sources should be carefully considered. Standby generators, back-up energy suppliers, or bulk energy storage systems may be necessary to alleviate the unbalancing issue caused by renewable energy fluctuation, which results in extra cost. In order to minimize the cost for obtaining extra energy and to increase energy efficiency, a flexible and efficient EV charging mechanism has to be properly designed to dynamically coordinate the renewable energy generation and energy demands of EVs.

In this chapter, we consider charging scheduling of a large number of EVs at a charging station which is equipped with renewable energy generation devices. The charging station can also obtain energy through controllable generators or buying

R. Wang et al., *Intelligent Microgrid Management and EV Control Under Uncertainties in Smart Grid*, https://doi.org/10.1007/978-981-10-4250-8_6

energy from outside power grid. Stimulated by the fact that in practical scenario, EV arrival and renewable energy may not follow any determinate process yet obtaining some statistical information of future EVs' arrivals (departures) is possible, we propose a novel two-stage EV charging mechanism to reduce the cost and efficiently utilize renewable energy. Several uncertain quantities such as the arrival and departure time of the EVs, their charging requirements and available renewable energies are all taken into account. In addition, the mechanism allows more information of EV arrivals (departures) and renewable energy generation to be effectively incorporated into the charging mechanism when such information is available. The main contributions of this chapter can be briefly summarized as follows:

- A day-ahead cost minimization problem is formulated and solved based on the available prediction of future renewable energy generation and EVs' arrivals (departures) to determine the amount of energy generated or imported in a day-ahead manner.
- We propose a real-time EV charging and power regulation scheme based on the planned energy generation day-ahead to determine the charging rate of each vehicle and power output adjustments in a dynamic and flexible manner.
- We develop a fast charging rate compression (CRC) algorithm which significantly reduces the complexity of solving the real-time EV charging scheduling problem. The proposed algorithm supports real-time operations and enables the large-scale small-step scheduling more efficiently.
- We further extend our mechanism to be applicable to two practical scenarios: (1) the charging station needs to track a given load profile; and (2) the EVs only have discrete charging rates.

Simulation results indicate that our proposed two-stage EV charging mechanism can effectively reduce the system expenditure and peak-to-average ratio (PAR). Moreover, the proposed mechanism enhances the system fault tolerance against renewable energy uncertainties and the noises of real-time data. Note that the proposed charging scheme adopts a universal methodology which is not restricted to the specific data traces used in the paper: as long as the renewable energy generation data and EVs pattern data (including EVs battery level, desired charging amount, charging speed, and arrival/departure times) can be obtained, the proposed EV charging scheduling scheme can be implemented with virtually no change.

The remainder of this chapter is organized as follows: Sect. 6.2 introduces the problem formulation and two-stage decision-making process. In Sect. 6.3, we present the fast charging compression algorithm. The simulation results and discussions are presented in Sect. 6.4. An extension of the proposed charging mechanism is discussed in Sect. 6.5. Finally, we conclude this chapter in Sect. 6.6.

6.2 Two-Stage Decision-Making Model and Problem Formulation

6.2.1 Two-Stage Decision-Making Model

As shown in Fig. 6.1, we consider a charging park where an intelligent controller is responsible for the charging scheduling of a large number of EVs. To meet the EVs' energy demands, the intelligent controller (1) acquires electricity from either controllable energy plants (a dedicated power supply [2]) or central power grid; and (2) harvests the renewable energy from local solar panels or wind turbines. Considering the practice of energy acquisition from controllable generators or power grid and the limited predictability of renewable energy, we propose a two-stage model for decision making as shown in Fig. 6.2. Specifically, at the first stage, we divide time into discrete time slots with equal length.[1] The preliminary energy acquisition profile $\tilde{E}_c(h)$ and energy transfer factor $\alpha(h)$ are determined day-ahead before dispatch based on the estimated EV energy demand $\tilde{E}_v(h)$ and renewable energy generation $\tilde{E}_r(h)$, where $h \in \mathcal{H}$ is the time slot index and $\mathcal{H}$ is the set of time slots in day-ahead scale. Note that $\tilde{E}_v(h)$ is computed through the EVs' arriving and departing pattern predictions. On the other hand, the supply of renewable power $P_r(t)$ and EVs' real power demand $P_v(t)$ at time t can only be known in real time, which requires the real-time control to balance the power supply and demand at the second stage (real-time stage) if necessary. Hence during the real-time EV charging scheduling, we try to obtain the proper EVs' charging rates $V_i(t)$ and real-time power acquisition $P_c(t)$ given the real-time renewable power generation $P_r(t)$, EVs' real-time parking profiles and day-ahead dispatched acquired power $\tilde{P}_c(t)$ (determined in the first stage). Note that for the first stage, the decision making is done one time day-ahead. For the second stage, it is done more frequently in real time, i.e., as long as the renewable power generation or the parking states change, the EVs' charging decision coordinates accordingly. Table 6.1 lists the main notations to be used in the rest of this chapter.

6.2.2 Modeling System Uncertainties

It can be noticed that the intelligent charging operation involves several uncertain quantities including power available from the renewable energy system, the EVs' arrival and departure time, and their required charging amount. These quantities are crucial parameters for managing the energy generation and consumption of the system. Although these quantities are random, there are good reasons to expect that

[1] For the day-ahead energy generation scheduling, the length of one time slot usually varies between 5 and 30 min (as indicated in p. 149, Ref. [3]). Typically, a smaller slot duration enables the energy generation scheduling more flexible; meanwhile it to a certain level complicated the computation process. The specific suitable time slot length depends on the scale of the charging system and accuracy of the demand and load predictions.

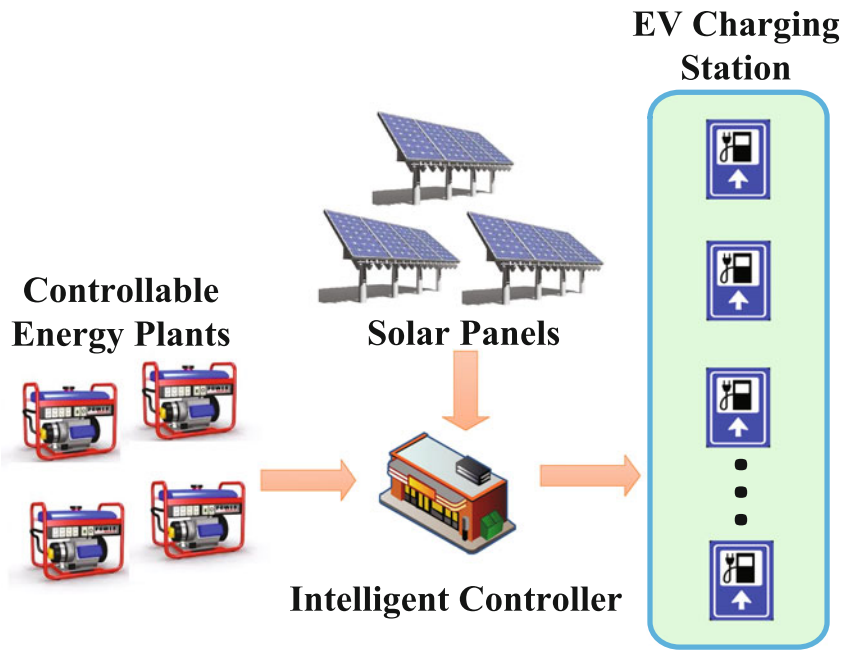

Fig. 6.1 The architecture of the EV charging station

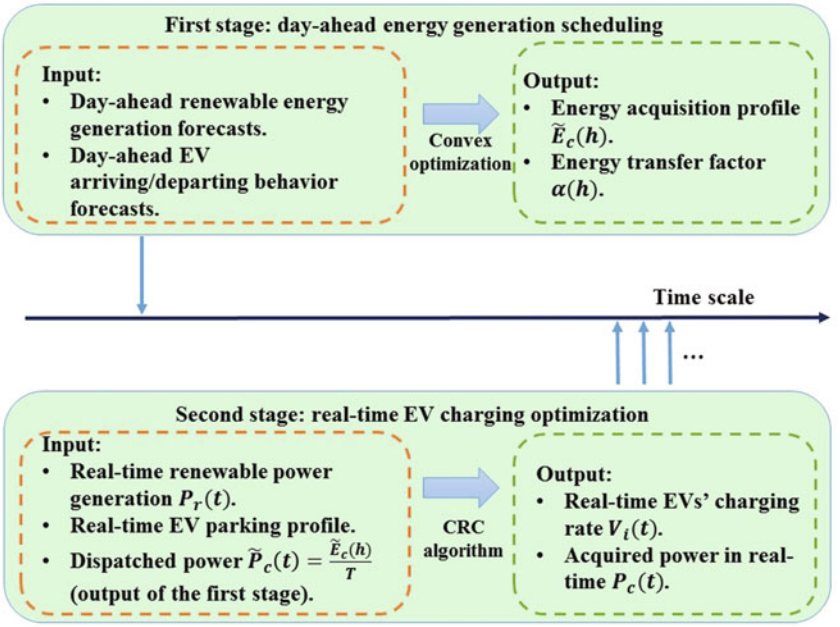

Fig. 6.2 Illustration of two-stage decision-making model. First stage (day-ahead): the decision variables are acquisition profile $\tilde{E_c}(h)$ and energy transfer factor $\alpha(h)$. Second stage (real-time): the decision variables are the charging speeds of EVs $V_i(t)$

Table 6.1 Notations used in this Chapter

Symbol	Definition
$\mathcal{H}$	Set of time slots in day-ahead scale, $\|\mathcal{H}\| = H$
h	Element in $\mathcal{H}$, time slot index in day-ahead scheduling
t	Time index in the real-time scheduling
$\tilde{E_c}(h)$	Predetermined energy acquisition at time slot h
$\tilde{E_v}(h)$	Estimated EV energy demand at time slot h
$\tilde{P_v}(t)$	Estimated EV power demand at time t
$\tilde{E_r}(h)$	Estimated renewable energy generation at time slot h
T	Length of one time slot
$\alpha(h)$	Energy transfer factor at time slot h
$M(t)$	The number of EVs in the charging park at time t
$w_i(t)$	Priority factor of EV i at time t
$V_{i_{max}}$	The maximum charging rate of EV i
$V_{i_{min}}$	The minimum charging rate of EV i
$V_i(t)$	Charging rate of vehicle i at time t
$V_d(t)$	The desired total charging demand at time t
$P_r(t)$	Renewable power realization at time t
$P_c(t)$	Power generated or imported in real-time
Γ	The set of charging tasks whose charging rates can vary
Γ_S	The set of charging tasks whose charging rates are fixed to maximum
τ_i	Charging task of EV i.

some statistical information may be obtained through accumulation of historical records. For example, the average energy generated by the renewable energy sources at each time slot can be estimated in a day-ahead manner based on the historical data and the weather forecast; inspecting a large number of samples of EVs' arrival and departure time, a probability distribution trend can be envisioned. We assume that the parking lot can roughly estimate the following parameters day-ahead: EVs arrival time distribution $f_A(x)$, departure time distribution $f_D(x)$, the total number of EVs being charged in a day $\bar{N}$, and the average charging rate of an EV μ_v. In this case, the estimated power (energy density) demand at time t can be expressed as:

$$\tilde{P_v}(t) = \int_0^t \big(f_A(x) - f_D(x)\big)\mathrm{d}x \cdot \bar{N} \cdot \mu_v, \tag{6.1}$$

and the estimated energy demand during time slot h is:

$$\tilde{E_v}(h) = \int_{h-1}^{h} \tilde{P_v}(t)\mathrm{d}t, \quad \forall h \in \mathcal{H}. \tag{6.2}$$

6.2.3 Day-Ahead Energy Acquisition Scheduling

The intelligent controller will firstly decide how much energy needs to be generated or imported in a day-ahead manner to minimize the expected energy acquisition cost while fulfilling the energy demand of EV charging station. The day-ahead energy acquisition scheduling problem can be formulated as:

$$\min_{\tilde{E}_c(h),\alpha(h)} \quad \sum_{h=1}^{H} \mathcal{C}_h\left(\tilde{E}_c(h)\right) \tag{6.3}$$

$$\text{s.t.} \quad \tilde{E}_c(h) + \tilde{E}_r(h) \geq \tilde{E}_v(h) \cdot \alpha(h) \tag{6.4}$$

$$\sum_{h=1}^{H} \tilde{E}_v(h) \cdot \alpha(h) = \sum_{h=1}^{H} \tilde{E}_v(h) \tag{6.5}$$

$$\alpha^L \leq \alpha(h) \leq \alpha^U, \forall h \in \mathcal{H}, \tag{6.6}$$

where $\mathcal{C}_h(\cdot)$ is the cost function of the electricity acquisition for the charging station, which is assumed to be an increasing convex function. The convex property reflects the fact that each additional unit of power needed to serve the demands is provided at a non-decreasing cost. Example cases include the quadratic cost function [4, 5] and the piecewise linear cost function [6, 7]. Without loss of generality, we consider quadratic cost function throughout this chapter. As to the renewable energy cost, for typical renewable energies (e.g., solar and wind energy), capital cost dominates. The operation and maintenance costs are typically very low or even negligible [8, 9]. In this chapter, it is assumed that the renewable energy generators such as solar panels and wind turbines have already been installed, and the marginal cost of renewable energy can be neglected, leading to its omission in the objective function [10]. Due to the flexibility of EVs' charging tasks, it is possible to shift some energy demand to other time slots to achieve the demand response target and reduce the total cost. $\alpha(h) > 0$ is an energy transfer factor, and $1 - \alpha(h)$ controls the portion of demand at time slot h shifted to other time slots. If $\alpha(h) > 1$, energy demand from other time slots is transferred to time slot h, whereas if $\alpha(h) < 1$, the energy demand in time slot h is shifted to other time slots. Note that $\alpha(h)$ can vary within its lower bound α^L and upper bound α^U. Constraint (6.4) is the load balance constraint, simply indicating that energy in each time slot should be balanced. Constraint (6.5) reveals the fact that the total energy required from EVs during a day remains unchanged, i.e., demand only transfers between time slots.

6.2.4 Real-Time Power Regulation and Elastic EV Charging

It is assumed that a two-way communication infrastructure (e.g., a local area network (LAN)) is available between the intelligent controller and vehicles. When an EV plugs

in, it informs the intelligent controller its unplug time, desired charging amount, maximum and minimum allowable charging rates. Also, it is assumed that the EV owners are rational, so that the desired charging amount will not exceed the maximum charging capacity of vehicle during its parking period. In other words, if the vehicle is charged at its maximum speed during the entire parking period, it can definitely reach the preset desired battery level. For the real-time operation, the intelligent controller has two tasks. First, given the real renewable generation and EVs' charging requirements, it has to determine a proper charging rate for each EV to achieve the optimal utilization of renewable energy and finish the charging tasks before EVs' departures. Second, the total acquired power should be properly regulated around the predetermined generation profile in real-time to match the fluctuant power demand, i.e., demand and supply should be balanced at any time instance.

From the standpoint of EV owners, it is desirable to reduce their EVs' charging time. For example, decreasing the charging time provides more flexibility for the owners to leave the charging station earlier. This objective can be captured by the constrained optimization problem as follows:

$$\min_{V_i(t)} \sum_{\tau_i \in \Gamma} w_i(t)\big(V_{i_{max}} - V_i(t)\big)^2, \tag{6.7}$$

$$\text{s.t.} \sum_{\tau_i \in \Gamma} V_i(t) + \sum_{\tau_i \in \Gamma_S} V_{i_{max}} \leq V_d(t), \tag{6.8}$$

$$V_i(t) \geq V_{i_{min}} \qquad \forall \tau_i \in \Gamma, \tag{6.9}$$

$$V_i(t) \leq V_{i_{max}} \qquad \forall \tau_i \in \Gamma. \tag{6.10}$$

In (6.7), decision variable is $V_i(t)$ which is the charging speed of EV i to be determined at time t. τ_i represents the charging task of vehicle i. Parameter $w_i(t) \geq 0$ is a priority factor which reflects the urgent degree of a charging task. More urgent tasks would have larger $w_i(t)$. Without loss of generality, $w_i(t)$ can be determined dynamically according to the state of the EV, which is defined as follows:

$$w_i(t) = \frac{E_i^r}{T_i^d - t}, \quad \forall \tau_i \in \Gamma, \tag{6.11}$$

where E_i^r is the amount of remaining requested energy for charging and T_i^d is EV i's departure time. Equation (6.11) indicates that urgent charging tasks will have a higher priority factor so as to be charged faster. This is to ensure that EVs depart with desired battery level. w_i also denotes the average charging rate EV i needs to finish the charging task τ_i on time. $V_{i_{max}}$ is the maximum charging rate (i.e., the desired charging rate) of EV i. $V_{i_{min}}$ is the minimum allowable charging rate of EV i. At any time t, the charging tasks can be first classified into two categories: Γ is the set of charging tasks whose charging rate can vary, i.e., $\Gamma = \{\tau_i |\ w_i(t) < V_{i_{max}}\}$. Γ_S denotes the set of charging tasks whose charging rates have to be fixed at the maximum charging rates because of the urgent charging time, i.e., $\Gamma_S = \{\tau_i |\ w_i(t) = V_{i_{max}}\}$. Note that elements in Γ and Γ_S may vary with time and for $\tau_i \in \Gamma$, $V_i \leq V_{i_{max}}$, for $\tau_i \in \Gamma_S$,

$V_i = V_{i_{max}}$. This EV classification approach ensures that all the EVs depart with satisfactory charging amount. $V_d(t)$ is the desired total charging demand at time t. The way to set $V_d(t)$ will be introduced later.

Notice that constraint (6.8) simply states the schedulability condition, and the rest of the constraints bound the charging rates. Due to EVs' arrivals and departures, the system is dynamic and the number of vehicles and their charging requirements will change over time. Therefore, the intelligent controller can solve problem (6.7)–(6.10) to obtain the charging rate for each EV at time t. When the renewable power realization changes, or an EV's status changes (τ_i changes from Γ to Γ_S) or a vehicle enters or departs the system, the intelligent controller will update Γ, Γ_S, and $V_d(t)$ in real time and then redo the calculation. Next, we will show how to determine $V_d(t)$ to optimally utilize the renewable energy.

Let $\tilde{P}_c(t) = \frac{\tilde{E}_c(h)}{T}$ denote the dispatched acquired power (i.e., the day-ahead pre-scheduled power generation) at time t, where T is the length of a time slot, and $P_r(t)$ denote the renewable generation realization at time t. Then, $V_d(t)$ can be defined as follows:

- If $\sum_{\tau_i \in \Gamma} V_{i_{min}} + \sum_{\tau_i \in \Gamma_S} V_{i_{max}} > \tilde{P}_c(t) + P_r(t)$, then $V_d(t) = \sum_{\tau_i \in \Gamma} V_{i_{min}} + \sum_{\tau_i \in \Gamma_S} V_{i_{max}}$, $P_c(t) = V_d(t) - P_r(t)$, $P_c(t)$ is the acquired power in real time. This is for the case where the renewable energy generation is very low, i.e., even though all the controllable EVs (EVs that belong to set Γ) charge at their minimum allowable charging rates, the demand is still higher than the available supply. Therefore, up regulation is required to guarantee the power balancing, i.e., more energy has to be imported, either by raising up the output level of fast-response generators or buying more electricity from ancillary service markets.
- If $\sum_{\tau_i \in \Gamma} V_{i_{min}} + \sum_{\tau_i \in \Gamma_S} V_{i_{max}} \le \tilde{P}_c(t) + P_r(t) \le \sum_{\tau_i \in \Gamma \cup \Gamma_S} V_{i_{max}}$, then $V_d(t) = \tilde{P}_c(t) + P_r(t)$ and $P_c(t) = \tilde{P}_c(t)$. This investigates the scenario where the renewable energy generation deviates not far from the previous prediction, i.e., the power demand of EVs can be adjusted to match the available supply. This represents the most common situation the charging system encounters. Under such case, the power demand of controllable EVs can be adjusted to match the supply, thus power acquisition profile does not need to be changed and is equal to the dispatched load determined day-ahead.
- If $\sum_{\tau_i \in \Gamma \cup \Gamma_S} V_{i_{max}} < P_r(t) + \tilde{P}_c(t)$, then $V_d(t) = \sum_{\tau_i \in \Gamma \cup \Gamma_S} V_{i_{max}}$ and $P_c(t) = \sum_{\tau_i \in \Gamma \cup \Gamma_S} V_{i_{max}} - P_r(t)$. This corresponds to the case where the renewable energy generation is plenty enough that even the highest charging demand can be satisfied, i.e., although all the EVs charge at the maximum charging rates, available power still exceeds. In this case, down regulation is required to make sure that power is balanced, i.e., the intelligent controller can reduce the acquired power level or sell the extra power out and only compensate the mismatch between the maximum charging demand and the renewable energy output.

Remark In day-ahead energy acquisition scheduling, the intelligent controller aims at minimizing the expected cost of the charging park given the estimated renewable energy supply $\tilde{E}_r(h)$ and EVs' energy demand $\tilde{E}_v(h)$, $h \in \mathcal{H}$. Decision variable

$\tilde{E}_c(h)$ is the scheduled electricity to be brought from day-ahead energy market or generated by base-load plants. In real-time power regulation, system reliability and EVs' charging requirements become the main concerns. The aforementioned up/down regulation is provided by ancillary service markets or fast-response generators [11].

6.3 The Charging Rate Compression Algorithm

The problems (6.7)–(6.10) belongs to the category of convex quadratic programs and can be solved in polynomial time. Many commercial optimization solvers including CPLEX, Mosek, FortMP, and Gurobi can be utilized to solve such problems. However, solving such a problem using quadratic program solver during run time can be still too costly, especially when the number of EVs is large and the response time has to be very short so as to quickly respond to EVs. What makes the above formulation attractive is that a charging rate compression (CRC) algorithm can be proposed such that the problem solving can be extremely fast. We first develop the CRC algorithm and then introduce a lemma and a theorem to prove that it can solve the problems (6.7)–(6.10).

At each time instance t, the set Γ of charging tasks can be further divided into two subsets: a set Γ_f of charging tasks with the minimum charging rate and a set Γ_v of charging tasks whose charging rate can still be compressed. Let $V_0 = \sum_{i\in\Gamma} V_{i_{max}}$ be the maximum power level of the charging task set Γ, V_{v_0} be the sum of maximum charging rates of charging tasks in Γ_v, and V_f be the sum of the charging rates of charging tasks in Γ_f. To achieve a desired power level $V_d(t) < V_0 + \sum_{i\in\Gamma_S} V_{i_{max}}$, each charging task has to be compressed up to the following charging rate:

$$\forall \tau_i \in \Gamma_v, \quad V_i = V_{i_{max}} - (V_{v_0} - V_m(t) + V_f)\frac{W_v}{w_i}, \tag{6.12}$$

where

$$V_m(t) = V_d(t) - \sum_{\tau_i\in\Gamma_S} V_{i_{max}} \tag{6.13}$$

$$V_{v_0} = \sum_{\tau_i\in\Gamma_v} V_{i_{max}} \tag{6.14}$$

$$V_f = \sum_{\tau_i\in\Gamma_f} V_{i_{min}} \tag{6.15}$$

$$W_v = \frac{1}{\sum_{\tau\in\Gamma_v}\frac{1}{w_i}}. \tag{6.16}$$

If there exist charging tasks where $V_i < V_{i_{min}}$, then the charging rates of these vehicles have to be fixed at their minimum value $V_{i_{min}}$. Sets Γ_f and Γ_v have to be updated (therefore, V_f, V_{v_0}, and W_v have to be recomputed), and (6.12) is applied again to

the charging tasks in Γ_v. If a feasible solution exists, i.e., the desired power level of the system is higher than or equal to the minimum power level $\sum_{i=1}^{M(t)} V_{i_{min}}$, the iterative process ends until each value computed by (6.12) is greater than or equal to its corresponding minimum $V_{i_{min}}$. The algorithm for compressing the charging rate of a set Γ of EVs to a desired charging power level $V_d(t)$ is shown in **Algorithm 6.1**.

Algorithm 6.1 Algorithm for compressing the charging rate for a charging task set of Γ at time t.

Input: $V_d(t)$, $V_{i_{min}}$, $V_{i_{max}}$, w_i, $\forall \tau_i \in \Gamma$.
Output: V_i, $\forall \tau_i \in \Gamma$.

Begin
$V_0 = \sum_{\tau_i \in \Gamma} V_{i_{max}}$;
$V_{min} = \sum_{\tau_i \in \Gamma} V_{i_{min}}$;
$V_m(t) = V_d(t) - \sum_{\tau_i \in \Gamma_S} V_{i_{max}}$;
if $(V_m(t) < V_{min})$
  Return INFEASIBLE;
else
  do {
    $\Gamma_f = \{\tau_i | V_i = V_{i_{min}}\}$;
    $\Gamma_v = \Gamma - \Gamma_f$;
    $V_{v_0} = \sum_{\tau_i \in \Gamma_v} V_{i_{max}}$;
    $V_f = \sum_{\tau_i \in \Gamma_f} V_{i_{min}}$;
    $W_v = \frac{1}{\sum_{\tau \in \Gamma_v} \frac{1}{w_i}}$;
    OK= 1;
    for (each $\tau_i \in \Gamma_v$)
      $V_i = V_{i_{max}} - (V_{v_0} - V_m(t) + V_f)\frac{W_v}{w_i}$;
      if $(V_i < V_{i_{min}})$
        $V_i = V_{i_{min}}$;
        OK= 0;
      end **if**
    end **for**
  } **while** (OK== 0);
  return FEASIBLE;
end **if**
End

Lemma 6.1 *Given the constraint optimization problem as specified in (6.7)–(6.10) and* $\sum_{\tau_i \in \Gamma} V_{i_{max}} > V_m(t)$, *any solution,* $V_i^*(t)$, *to the problem must satisfy* $\sum_{\tau_i \in \Gamma} V_i^*(t) = V_m(t)$ *and* $V_i^*(t) \neq V_{i_{max}}$, *for all* $\tau_i \in \Gamma$.

Theorem 6.1 *Given the constraint optimization problem as specified in (6.7)–(6.10),* $\sum_{\tau_i \in \Gamma} V_{i_{max}} > V_m(t)$, *and* $\sum_{\tau_i \in \Gamma} V_{i_{min}} < V_m(t)$, *let* $\widehat{V}(t) = \sum_{V_i^*(t) \neq V_{i_{min}}} V_{i_{max}} + \sum_{V_i^*(t) = V_{i_{min}}} V_{i_{min}}$. *A solution is optimal if and only if*

$$V_i^*(t) = V_{i_{max}} - \frac{\frac{1}{w_i(t)}(\widehat{V}(t) - V_m(t))}{\sum_{V_j^*(t) \neq V_{j_{min}}} (1/w_j)}, \tag{6.17}$$

for $\widehat{V}(t) > V_m(t)$ *and* $V_i^*(t) > V_{i_{min}}$, *and* $V_i^*(t) = V_{i_{min}}$ *otherwise.*

The proofs of Lemma 6.1 and Theorem 6.1 are given in the **Appendix B**. Based on the previous lemma and theorem, we can draw the conclusion as follows:

Corollary 6.1 *Consider the charging tasks of* $|\Gamma \cup \Gamma_S|$ *EVs, where* $V_i(t)$ *is the charging rate of the* i*th vehicle. Let* $V_{i_{max}}$ *denote the initial desired charging rate of charging task* $\tau_i \in \Gamma \cup \Gamma_S$ *and* $w_i(t)$ *be the set of priority factors. Let* $V_d(t)$ *be the desired power level of the system and* $\sum_{\tau_i \in \Gamma} V_{i_{max}} > V_m(t)$. *The charging rate* V_i, $\tau_i \in \Gamma$, *obtained from* ***Algorithm 6.1*** *minimizes*

$$\sum_{\tau_i \in \Gamma} w_i(t)\big(V_{i_{max}} - V_i(t)\big)^2$$

subject to the inequality constraints $\sum_{\tau_i \in \Gamma} V_i(t) + \sum_{\tau_i \in \Gamma_S} V_{i_{max}} \leq V_d(t)$, $V_i(t) \geq V_{i_{min}}$, *and* $V_i(t) \leq V_{i_{max}}$ *for* $\tau_i \in \Gamma$.

Remark Through analysis, the time complexity of **Algorithm 6.1** is $O(n^2)$, where n is the number of tasks in Γ.

6.4 Simulation Results and Discussions

In this section, we present simulation results based on real-world traces for assessing the performance of the proposed two-stage EV charging scheme.

6.4.1 Parameters and Settings

We assume there are solar panels providing renewable energy for the charging station. The area of the solar panels in the system is set to be $3.125 \times 10^4\ \mathrm{m}^2$. The energy conversion efficiency is 0.8. The solar radiation intensity statistic is adopted from [12], from which we employ the solar radiation data of a typical day in winter (17/01/2013). The data utilized for the day-ahead energy acquisition scheduling and real-time EV charging are depicted in Fig. 6.3. Note that the predicted average solar radiance utilized in the day-ahead energy generation scheduling is plotted in the blue circled line, and the actual real-time solar radiance adopted in the real-time charging is shown by the red curve. We envision the scenario that the charging station is located at a workplace (e.g., a campus) that is active from 6:00 AM to 6:00 PM. Vehicles arrive earlier than 6:00 AM start to charge at 6:00 AM while those depart later than 6:00 PM finish their charging before 6:00 PM. We simulate the operation process of a large-scale charging station which serves totally 3000 EVs arriving and departing independently in a typical day. It is assumed that the arrival time distribution and departure time distribution are all Gaussian with parameters shown in Table 6.2

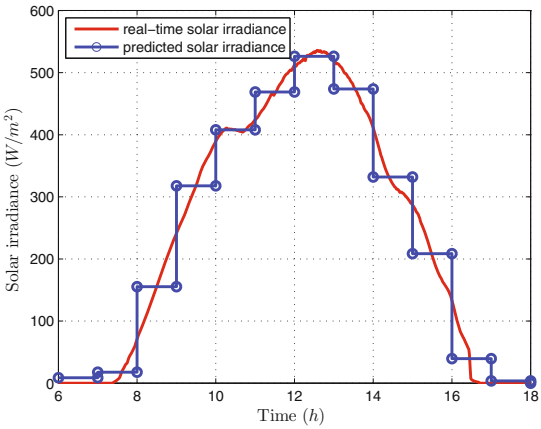

Fig. 6.3 Solar irradiance in a day

Table 6.2 Parameters of the arrival and departure time probability distribution

Time parameter	Arrival	Departure
Mean: μ_r	10	14
Standard deviation: σ_r	1.2	1.3

(similar assumptions can be found in many papers, e.g., [13, 14]). EVs are active for charging during their parking time, and discharging is not permitted. The amount of energy needed for the EVs are evenly distributed between 20 KWh and 50 KWh. The maximum allowable charging rate of an EV is 62.5 KW (e.g., high-voltage (up to 500 VDC) high-current (125 A) automotive fast charging [15]), and the minimum charging rate of an EV is 0 KW. The cost function of the electricity acquisition is $\mathcal{C}_h\left(\tilde{E}_c(h)\right) = a_h \cdot \tilde{E}_c(h)^2$ and $a_h = 150\ \$ \cdot (\text{MWh})^{-2}$.

6.4.2 *Results and Discussions*

The simulation process contains two parts. First, given the estimated solar energy in each time slot (in the simulation, one time slot is set as one hour), we solve the day-ahead energy acquisition scheduling problems (6.3)–(6.6) and obtain $\tilde{E}_c(h)$ and $\alpha(h)$ for $h = 1, \ldots, H$. The upper bound and lower bound of energy transfer parameter $\alpha(h)$ is set to be 2 and 0.5, respectively. Once the dispatched energy acquisition in each time slot is obtained, we are ready to simulate the charging process of EVs based on the real-time renewable power generation and EVs' real-time arrival (departure) patterns. Adopting the data previously mentioned, all the simulations are conducted on an Intel workstation with six processors clocking at 3.2 GHZ and 16 GB of RAM. We repeated the simulation for 10 times. All the 3000

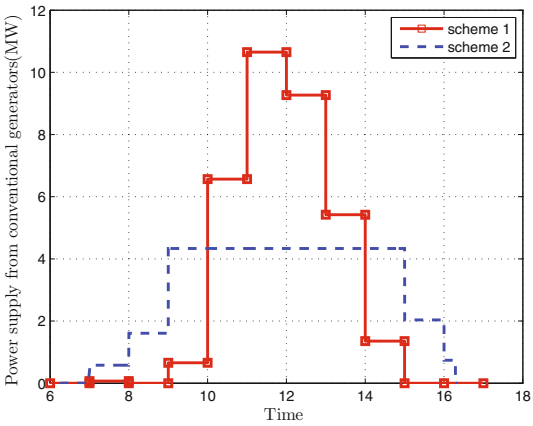

Fig. 6.4 Energy supply from conventional generators under different charging schemes

EVs complete charging with required amount before their departures. By utilizing the CRC algorithm introduced in Sect. 6.3, the simulation time is reduced from 1005.1 s to 101.2 s, showing that the proposed CRC algorithm can significantly reduce the complexity of the problem solving. Note that our CRC algorithm does not sacrifice the problem-solving accuracy, and we obtain exactly the same results when adopting quadratic programming solvers and our CRC algorithm.

We first investigate the effectiveness of our proposed EV charging mechanism. Specifically, two charging schemes are compared. In the first scheme, EVs are kept charging during their parking time and the charge speeds are the average rates that they need to fulfill the charging tasks. Conventional generators generate electricity for the unbalanced power demand in an on-demand manner. While in the second scheme, the charging station charges EVs' batteries according to the mechanism we proposed, and electricity is generated based on the day-ahead scheduling and real-time adjustment. The simulation results concerning the power supply curves, total system cost, and peak-to-average ratio (PAR) under these two schemes are given in Figs. 6.4 and 6.5, respectively. As we mentioned previously, quadratic cost functions are adopted to compute the system expenditures for both schemes.

In Fig. 6.4, it is shown that by optimally controlling the charging rates of EVs, our proposed charging strategy successfully transfers the peak demand to the off-peak hours, which can help stabilize the operations of the charging system and reduce the energy cost. As shown in Fig. 6.5, the total expenditure of the charging station decreases from $\$4.1 \times 10^4$ per day in scheme 1 to $\$1.8 \times 10^4$ per day in our proposed scheme, achieving a cost saving of 56.1%. Therefore, one of the aims of the developed charging strategy, which is reducing the expenditure of the system, is achieved. To investigate the variation of PAR, we study two cases: (1) PAR of the aggregated supply (i.e., the supply from controllable generators plus the supply from solar panels); and (2) PAR of the controllable generators' output. As we observe in Fig. 6.5, with scheme 1, the PAR of the aggregated supply and the PAR of controllable generators' output are 2.69 and 3.95, respectively. By adopting the proposed charging

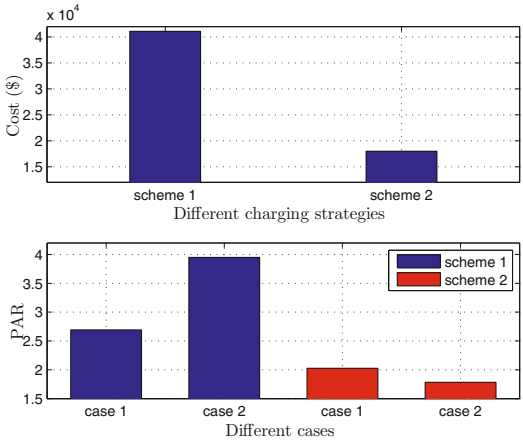

Fig. 6.5 Cost and PAR comparisons of different charging schemes

scheme, these two PAR values reduce to 2.02 and 1.78 (decrease about 25 and 55%), respectively. The proposed EV charging strategy presents much better PAR performance during the 12-h operation. An interesting observation is that in scheme 1, the PAR of controllable generators' output is much higher than that of the aggregated power supply; however, the situation is exactly opposite in our proposed scheme. In other words, under normal circumstances, utilizing renewable energy will make the output of controllable generators more fluctuant, whereas EVs can help solve this problem by properly varying their charging speeds, i.e., charging quickly when renewable energy is sufficient and reducing the rate when not enough renewable energy is available.

In our scheme, the first-stage day-ahead energy generation scheduling is based on the estimated renewable energy generation in next day. Normally, the real renewable energy generation might be different from the estimated one. Next, we investigate the cost sensitivity with respect to this deviation. The simulation results are depicted in Fig. 6.6. Specifically, we conduct the experiment as follows. In the first step, the day-ahead energy generation scheduling is done based on the estimated solar irradiance and EVs' arriving (departing) patterns. Then, for the real-time charging, we vary the solar irradiance data based on the real-world trace to represent different estimation error levels. As it is observed in Fig. 6.6, system cost is much more sensitive in scheme 1 than that in our scheme when the deviation varies. The reason is that by applying our charging strategy, deviations of the solar power can be distributed to the whole time horizon. However in scheme 1, the situation that solar power is excessive during some time periods and insufficient in some other time becomes more severe. Under such case, solar energy utilization efficiency fluctuates more extensively when deviation level increases, and accordingly, system cost varies more violently. Hence, our charging mechanism can effectively reduce the financial risks caused by the estimation error of the renewable energy generation.

Figure 6.7 illustrates how system cost varies under different fluctuation levels of solar energy. In this experiment, we add 0-mean Gaussian noise to the real-time solar

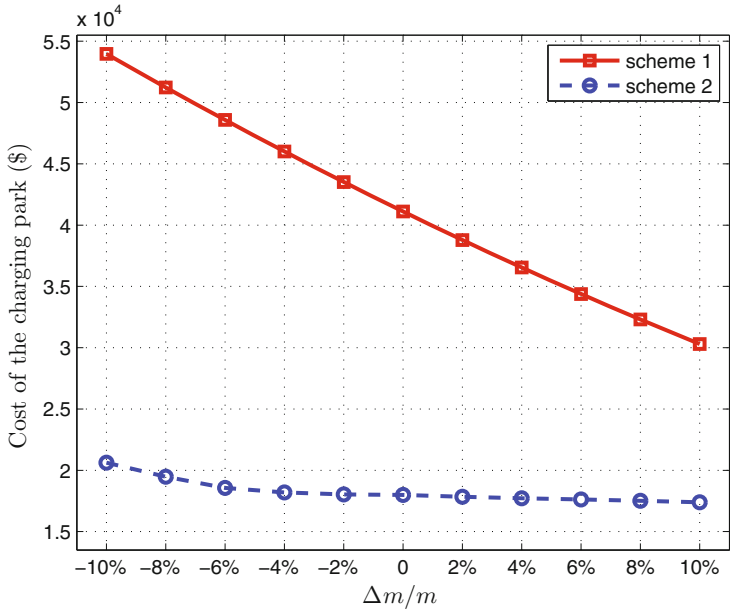

Fig. 6.6 System cost with respect to the real-time renewable generation deviation (Δm represents the deviation of real solar irradiance from the estimated one, and m is the actual data trace)

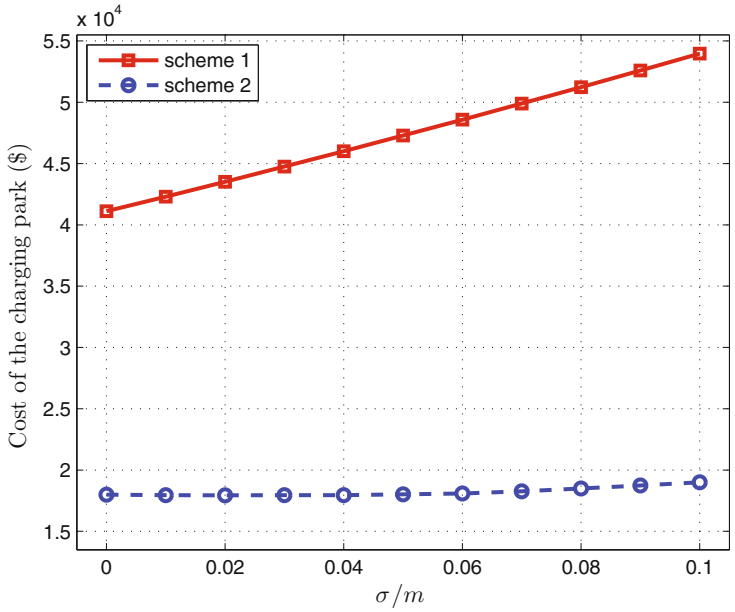

Fig. 6.7 System cost with respect to the different fluctuation level of renewable energy (m represents the actual data trace, and σ represents the standard deviation of noise)

irradiance data and then evaluate its impact on the system cost. Different standard deviations of the noise reflect different fluctuation levels of solar energy. It appears that the fluctuation of renewable energy has less impact on the system cost when adopting our proposed scheduling scheme. This observation is intuitive since by properly altering their charging rates, EVs act as an energy storage which may to a certain extent alleviate the uncertainty problem. However in scheme 1, the controllable generators have to compensate the solar power fluctuation during the entire time horizon. In this case, the system cost will be affected more extensively when fluctuation level increases. Note that this experiment also simulates the scenario that system data is affected by noises. Thus, we claim that the our proposed EV charging mechanism shows good performances in dealing with uncertainties of renewable energy and noises of real-time data.

6.5 Extensions

6.5.1 Tracking a Given Load Profile

The electricity utilized for EV charging can be provided by a utility company. The objective of the utility company may be to flatten the total load profile. The utility company may also need to buy electricity in day-ahead electricity market and supply the electricity to the charging parking as well as other energy consumers in real-time. Under such case, the utility company may want the charging station to properly schedule the charging of EVs, so that the demand can track the electricity profile it brought in the day-ahead electricity market. Denote the load profile that the charging park tracks as $L(t)$. Our charging scheme can be extended to track $L(t)$ by solving the following constraint optimization problem:

$$\min_{V_i(t)} \sum_{\tau_i \in \Gamma} w_i(t)\left(V_{i_{max}} - V_i(t)\right)^2, \tag{6.18}$$

$$\text{s.t.} \sum_{\tau_i \in \Gamma} V_i(t) + \sum_{\tau_i \in \Gamma_S} V_{i_{max}} \leq L(t), \tag{6.19}$$

$$V_i(t) \geq V_{i_{min}} \qquad \forall \tau_i \in \Gamma, \tag{6.20}$$

$$V_i(t) \leq V_{i_{max}} \qquad \forall \tau_i \in \Gamma. \tag{6.21}$$

Figure 6.8 shows the simulation results of tracking given target load profiles. The intelligent controller is in charge of managing 3000 EVs in a day on their charging schedules. These vehicles plug in uniformly distributed between 6:00 and 14:00, with deadlines uniformly distributed between 10:00 and 18:00. The amount of energies needed to charge are evenly distributed between 20 KWh and 50 KWh. Two testings are conducted to show the load tracking results with different target profiles. The target profiles are represented by the blue dot-circled curves. The red

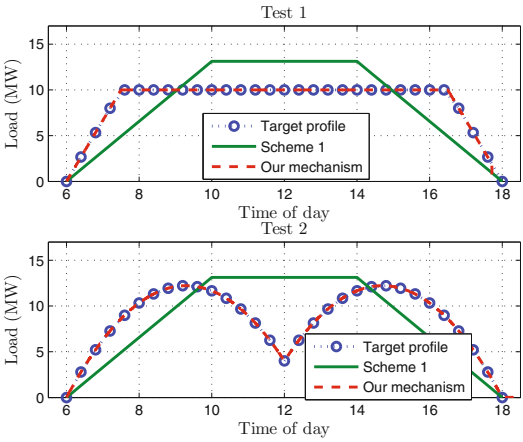

Fig. 6.8 Tracking given target load profiles

dash curves and green solid curves correspond to the aggregated charging rates obtained from our EV charging mechanism and scheme 1, respectively. We observe that the aggregated charging demand can closely follow the target load profiles when adopting our proposed charging scheme. There are only small discrepancies around 18:00 due to the early or late departures of EVs.

Remark In order to ensure that the electricity demand of EVs can closely follow the target load profile, load profile $L(t)$ should not go beyond the variation limits of EVs' charging rates, that is:

$$L(t) \geq \sum_{\tau_i \in \Gamma} V_{i_{min}} + \sum_{\tau_i \in \Gamma_S} V_{i_{max}} \tag{6.22}$$

and

$$L(t) \leq \sum_{\tau_i \in \Gamma} V_{i_{max}} + \sum_{\tau_i \in \Gamma_S} V_{i_{max}} \tag{6.23}$$

6.5.2 Discrete Charging Rates

In our proposed charging scheme, we assume that the charging rate can vary continuously within the EV's maximum and minimum allowable rates, determined by the charger. Similar assumptions can be found in many literature including [16–18]. However in some circumstances, if only a few discrete charging speeds are allowed, the proposed EV charging scheme can be easily extended to handle such case. Let $\mathcal{V}_i$ denote the set of allowable charging rates of vehicle i. To capture the discrete charging rate case, we replace constraints (6.9) and (6.10) with the following constraint in

Table 6.3 Simulation results under continuous charging rate case and discrete charging rate case (all results are 10 times average)

Charging park size	Power level type	Charging cost ($)	Cost growth (%)
Large scale (3000 EVs)	Continuous charging rate case	17993.1	–
	Discrete charging rate case	18028.8	0.2
Medium scale (500 EVs)	Continuous charging rate case	497.1	–
	Discrete charging rate case	511.2	2.8
Small scale (100 EVs)	Continuous charging rate case	22.2	–
	Discrete charging rate case	27.9	25.7

real-time EV charging:

$$V_i(t) \in \mathcal{V}_i \qquad \forall \tau_i \in \Gamma. \tag{6.24}$$

Although the CRC algorithm is only suitable for the continuous charging rate case, simulations show that with discrete allowable charging rates, the proposed two-stage charging mechanism still has an acceptable computation-time performance. In the simulation, each EV has four allowable charging speeds, i.e., $\mathcal{V}_i = \{0 \text{ KW}, 20 \text{ KW}, 40 \text{ KW}, \text{ and } 62.5 \text{ KW}\}, \forall \tau_i \in \Gamma$ [2]. The number of EVs served in a day is still 3000. The simulation results comparison with the continuous charging rate case is summarized in the first row of Table 6.3. Note that the simulations under both cases are conducted 10 times, and results in Table 6.3 are the average.

As it is shown in Table 6.3, two main observations can be found as follows:

- For the discrete charging rate case, though the simulation time is much longer for the continuous charging rate case, our two-stage EV charging mechanism still performs acceptably for the real-time scheduling since computation time for updating the charging rates of active vehicles is about 0.25 s on average. Note that this is the updating time running on the computer whose configuration is specified in the previous subsection.
- The system cost increases slightly (about 0.2%) when only several discrete charging rates are allowed. This observation is intuitive since with discrete charging rates, the scheduling flexibility is abated and mechanism performance gets worse. In other words, when EVs' charging rates can vary continuously, the power demand can follow the desired power supply more closely and thus utilize the renewable energy in a more efficient manner. However, since the number of EVs is large, discrepancy between the combinations of EVs' discrete charging rates and desired energy supply level is not significant. Thus, the cost only increases slightly.

We further reduce the simulation scale to medium size (e.g., 500 vehicles) and small size (e.g., 100 vehicles) to investigate how the size of the charging park impacts the performances of the proposed scheme. Besides the charging park size, simulation process and system parameters are exactly the same to those in the previous subsection. The area of the solar panels varies proportionally with the charging park size. We also simulate 10 times and the results' data are depicted in Table 6.3. It appears that for large-, medium-, and small-scale charging parks, system costs in discrete charging rate case are 0.2, 2.8, and 25.7% higher than those in the continuous charging rate case, respectively. In other words, system cost is more sensitive to the discrete charging rate condition when the scale of charging park shrinks. The reason for this phenomenon is that when the number of connected vehicles gets small and only several discrete charging rates are allowed, the flexibility of the system deteriorates. There will be a higher probability that aggregated charging demand cannot match the available power. For instance, when there are only 30 KW power available and two vehicles are active at a given time, for the continuous charging rate case, EVs are able to follow the supply closely. Whereas for the discrete charging rate case, either 10 KW power is wasted or conventional units have to generate 10 KW more so that discrete demand can be matched. Therefore, power utilization becomes less efficient, and conventional generators have to produce more electricity to ensure that charging tasks can be finished in time. As we mentioned previously, when the number of EVs is large, discrepancy between the combinations of EVs' discrete charging rates and desired energy supply level becomes less significant, leading to only marginal increase in cost. The proposed EV charging scheme favors reasonably for a large charging park when only discrete charging rates are allowed.

6.6 Conclusion

In this chapter, we investigate the cost-effective scheduling approach of EV charging at a renewable energy aided charging station. We design a two-stage EV charging scheme to determine energy generation and charging rates of EVs. Specifically, at the first stage, based on the EV pattern and renewable energy generation estimation, a cost minimization problem is formulated and solved to obtain a preliminary energy generation or importation scheduling profile in a day-ahead manner. Then at the second stage, a real-time EV charging and power regulation scheme are proposed. Such a scheme allows convenient handling of volatile renewable energy and indeterminate EV patterns. We also develop an efficient charging compression algorithm to further lower the complexity of the problem solving. Simulation results indicate the satisfactory efficiency of the proposed EV charging mechanism and the cost benefits obtained from it. Moreover, the impacts of renewable energy uncertainties have been carefully evaluated. The results show that the proposed EV charging scheme has a good performance in enhancing the system fault tolerance against uncertainties and the noises of real-time data. Such evaluations, as we believe, reveal that the proposed charging mechanism is suitable for the case with a large number of EVs and

unstable renewable energy. Furthermore, we extend the mechanism to track a given load profile and handle the scenario that EVs only have discrete charging rates. As a universal methodology, the proposed scheme is not restricted to any specific data traces and can be easily applied to many other cases as well.

References

1. D.B. Richardson, Electric vehicles and the electric grid: a review of modeling approaches, impacts, and renewable energy integration. Renew. Sustain. Energy Rev. **19**, 247–254 (2013)
2. F. Mwasilu, J.J. Justo, E.-K. Kim, T.D. Do, J.-W. Jung, Electric vehicles and smart grid interaction: a review on vehicle to grid and renewable energy sources integration. Renew. Sustain. Energy Rev. **34**, 501–516 (2014)
3. C. Harris, *Electricity Markets: Pricing, Structures and Economics* (Wiley, New York, 2006)
4. A. Mohsenian-Rad, V. Wong, J. Jatskevich, R. Schober, A. Leon-Garcia, Autonomous demand-side management based on game-theoretic energy consumption scheduling for the future smart grid. IEEE Trans. Smart Grid **1**(3), 320–331 (2010)
5. P. Samadi, H. Mohsenian-Rad, R. Schober, V. Wong, Advanced demand side management for the future smart grid using mechanism design. IEEE Trans. Smart Grid **3**(3), 1170–1180 (2012)
6. C. Joe-Wong, S. Sen, S. Ha, M. Chiang, Optimized day-ahead pricing for smart grids with device-specific scheduling flexibility. IEEE J. Sel. Areas Commun. **30**(6), 1075–1085 (2012)
7. I. Koutsopoulos, L. Tassiulas, Optimal control policies for power demand scheduling in the smart grid. IEEE J. Sel. Areas Commun. **30**(6), 1049–1060 (2012)
8. Renewable power generation costs in 2012: an overview (2012)
9. Handbook for solar photovoltaic (pv) systems (2011)
10. Y. Guo, M. Pan, Y. Fang, Optimal power management of residential customers in the smart grid. IEEE Trans. Parallel Distrib. Syst. **23**(9), 1593–1606 (2012)
11. B. Kirby, Ancillary services: Technical and commercial insights. Retrieved October, vol. 4, p. 2012 (2007)
12. Nrel: National renewable energy laboratory (2013)
13. C. Jin, X. Sheng, P. Ghosh, Energy efficient algorithms for electric vehicle charging with intermittent renewable energy sources. In *IEEE Power and Energy Soc. General Meeting*, pp. 1–5, IEEE (2013)
14. A. Mohamed, V. Salehi, T. Ma, O. Mohammed, Real-time energy management algorithm for plug-in hybrid electric vehicle charging parks involving sustainable energy. IEEE Trans. Sustain. Energy **5**(2), 577–586 (2014)
15. Chademo: Dc fast charging
16. W. Tang, S. Bi, Y.J. Zhang, Online speeding optimal charging algorithm for electric vehicles without future information. In *IEEE International Conference on Smart Grid Communications*, pp. 175–180, IEEE (2013)
17. Z. Ma, D. Callaway, I. Hiskens, Decentralized charging control for large populations of plug-in electric vehicles. In *IEEE Annual Conference on Decision and Control*, pp. 206–212, IEEE (2010)
18. L. Gan, U. Topcu, S. Low, Optimal decentralized protocol for electric vehicle charging. IEEE Trans. Power Syst. **28**(2), 940–951 (2013)